52 *Organometallics* **1990**, *9*, 52-59

Synthesis, Structure, and Fluxional Properties of $[(OC)_4(Bu^tNC)Os]Os_3(CO)_{11}$. Evidence for Restricted Rotation about a Metal–Metal Bond

Frederick W. B. Einstein,* Victor J. Johnston, Andrew K. Ma, and Roland K. Pomeroy*

Department of Chemistry, Simon Fraser University, Burnaby, British Columbia, Canada V5A 1S6

Received March 21, 1989

The cluster $Os_4(CO)_{15}(CNBu^t)$ (1) has been prepared by the addition of Bu^tNC to $Os_4(CO)_{15}$ in CH_2Cl_2 at 0 °C. The structure of 1 has been solved by X-ray crystallography: space group $P2/a$ with a = 15.946 (2) Å, b = 11.465 (2) Å, c = 16.776 (2) Å, β = 92.09 (1)°, V = 3064.8 Å^3, Z = 4; R_1 = 0.051, R_2 = 0.057 for 2163 observed reflections; there is a partial molecule of CH_2Cl_2 that is disordered. In 1, the 18-electron compound $Os(CO)_4(CNBu^t)$ acts as a ligand to the $Os_3(CO)_{11}$ fragment via an unbridged dative Os–Os bond of length 2.918 (2) Å; the Bu^tNC ligand is cis to this bond. The Os–Os bond lengths within the Os_3 triangle are 2.853 (2) Å (trans to the dative Os–Os bond), 2.929 (2) Å (cis to the dative Os–Os bond), and 2.890 (2) Å. The ^{13}C NMR spectrum of 1 in solution at −118 °C is consistent with a rigid structure in which the Bu^tNC ligand is locked to one side of the Os_4 plane. As the temperature is raised, sets of signals in the spectrum collapse to the base line at different rates such that at 0 °C only one signal remains sharp. This fluxional behavior is interpreted in terms of an initial rapid oscillation of the isocyanide ligand about the Os_4 plane, followed at higher temperatures by various carbonyl exchanges that involve all the carbonyls except that which is trans to the isocyanide ligand. The synthesis and fluxional properties of [*cis*-$(OC)_3(Bu^tNC)_2Os]Os_3(CO)_{11}$ (2) are also described. Interestingly, for 2 in solution, the carbonyls of the $Os(CO)_3(CNBu^t)_2$ ligand do not undergo exchange with the carbonyls of $Os_3(CO)_{11}$ unit even at room temperature.

Introduction

We have recently described the synthesis and structure of the 64-electron clusters $Os_4(CO)_{16}$ (3)[1] and $Os_4(CO)_{15}(PMe_3)$ (4).[2] As expected from polyhedral skeletal electron pair theory[3] both clusters have four metal–metal bonds, however, whereas 3 has a cyclobutane-like Os_4 core, 4 has a spiked triangular skeleton with a dative metal–metal bond (i.e., $[(Me_3P)(OC)_4Os]Os_3(CO)_{11}$). The reason for the different structures is not clear. We have therefore initiated an investigation into the synthesis of derivatives of the type $Os_4(CO)_{15}(L)$ (L = two-electron donor ligand) in an attempt to clarify why a particular structure is adopted.

Here we report the synthesis of $Os_4(CO)_{15}(CNBu^t)$ (1) and $Os_4(CO)_{14}(CNBu^t)_2$ (2). The X-ray crystal structure of 1 reveals it to have a spiked triangular geometry, a structure also believed to be adopted by 2. Also reported here, and of equal interest, are the variable-temperature ^{13}C NMR spectra of the clusters that indicate a number of different fluxional processes occur in each molecule in solution below 0 °C. The mode of collapse of the signals in the lowest energy process of 1 is consistent with oscillation about the dative Os–Os bond.

Experimental Section

Manipulations of starting materials and products were carried out under a nitrogen atmosphere with the use of Schlenk techniques. Hexane was refluxed over potassium, distilled, and stored under nitrogen before use. Dichloromethane was treated similarly except that P_2O_5 was used as the drying agent. The preparations of the starting materials $Os_4(CO)_{14}$[4] and $Os_4(CO)_{15}$[5] have been briefly described; more detailed preparations will be submitted for publication in the near future. The ^{13}CO-enriched compounds were obtained from ^{13}CO-enriched $Os_3(CO)_{12}$ (~35% ^{13}C) which was prepared by heating $Os_3(CO)_{12}$ in toluene at 125 °C under ~1.5 atm of ^{13}CO (99% ^{13}C) for 3 days.

Infrared spectra were recorded on a Perkin-Elmer 983 spectrometer; the internal calibration of the instrument was periodically checked against the known absorption frequencies of gaseous CO. NMR spectra were recorded on a Bruker WM400 spectrometer. The spectra shown in Figures 2–5 were obtained on 10–15 mg of ^{13}CO-enriched sample in ~0.75 mL of solvent and are the result of the accumulation of 700–3500 FID's. The melting point was determined on a sample sealed in a capillary in air by use of a Mel-temp apparatus. Microanalyses were performed by M. K. Yang of the Microanalytical Laboratory of Simon Fraser University.

Preparation of $Os_4(CO)_{15}(CNBu^t)$ (1). To a solution of $Os_4(CO)_{15}$ (73 mg, 0.062 mmol) in CH_2Cl_2 (25 mL) at 0 °C, Bu^tNC in hexane (ca. 1 mg/mL) was added dropwise until the color of the solution had just changed from dark green to bright orange. An infrared spectrum (CO region) of the solution at this stage showed no absorptions due to $Os_4(CO)_{15}$. The solvent and excess Bu^tNC were removed on the vacuum line, and the residue was recrystallized from CH_2Cl_2–hexane to give orange, air-stable $Os_4(CO)_{15}(CNBu^t)$ (69 mg, 88%): mp 118 °C; IR (CH_2Cl_2) ν(CN) 2222.5 (m), ν(CO) 2120 (m), 2088 (s), 2060 (sh), 2049 (vs), 2041 (sh), 2007 (vs, br), 1974.5 (m), 1960 (w), 1915 (m) cm^{-1}; ^1H NMR (C_6D_6, 21 °C) δ 0.78 (Bu^t); ^{13}C NMR (CO region; $CHFCl_2/CD_2Cl_2$; −118 °C) δ 199.2, 198.7, 188.2, 187.8, 184.6 (2 C), 184.3, 179.9, 178.8, 177.0, 174.9, 173.4, 171.9, 171.0, 160.4; 1 did not give a satisfactory (EI) MS. Anal. Calcd for $C_{20}H_9NO_{15}Os_4$: C, 19.00; H, 0.72; N, 1.11. Found: C, 19.29; H, 0.82; N, 1.09. The X-ray structure of 1 revealed a partial molecule of CH_2Cl_2 (see below). That this is not indicated in the elemental analysis of 1 suggests that CH_2Cl_2 was removed during the thorough drying of the analytical sample before analysis.

Preparation of $Os_4(CO)_{14}(CNBu^t)_2$ (2). To a solution of $Os_4(CO)_{14}$ (11 mg, 9.5 × 10^{-3} mmol) in CH_2Cl_2 (15 mL) was added a solution of $CNBu^t$ in hexane dropwise until the solution changed to bright yellow-orange. The progress of the reaction was also monitored by the disappearance of the band at 2055 cm^{-1} in the infrared spectrum of the original solution. Solvent and excess $CNBu^t$ were removed on the vacuum line. The remaining solid was recrystallized from CH_2Cl_2–hexane to yield orange, air-stable crystals of $Os_4(CO)_{14}(CNBu^t)_2$ (8 mg, 63%): IR (CH_2Cl_2) ν(CN) 2220.5 (w), 2201.5 (w), ν(CO) 2095.5 (m), 2067 (s), 2039 (s), 2005 (s, br), 1967.5 (w), 1956 (sh), 1906 (w) cm^{-1}; ^1H NMR (C_7D_8, 25

---

(1) Johnston, V. J.; Einstein, F. W. B.; Pomeroy, R. K. *J. Am. Chem. Soc.* **1987**, *109*, 8111.

(2) Martin, L. R.; Einstein, F. W. B.; Pomeroy, R. K. *Organometallics* **1988**, *7*, 294.

(3) (a) Wade, K. In *Transition Metal Clusters*; Johnson, B. F. G., Ed.; Wiley: Chicester, England, 1980; p 183. (b) Mingos, D. M. P. *Acc. Chem. Res.* **1984**, *17*, 311. (c) Johnson, B. F. G.; Benfield, R. E. *Top. Stereochem.* **1981**, *12*, 253.

(4) Johnston, V. J.; Einstein, F. W. B.; Pomeroy, R. K. *Organometallics* **1988**, *7*, 1867.

(5) Johnston, V. J.; Einstein, F. W. B.; Pomeroy, R. K. *J. Am. Chem. Soc.* **1987**, *109*, 7220.

Table I. Summary of Crystal Data for $Os_4(CO)_{15}(CNBu^t) \bullet 0.4CH_2Cl_2$

fw	1297.4
color	orange-yellow
space group	*P*2/*a*
cryst syst	monoclinic
temp, °C	22
a, Å	15.946 (2)
b, Å	11.465 (2)
c, Å	16.776 (2)
β, deg	92.09 (1)
V, $Å^3$	3064.8
Z	4
d_{calcd}, g cm^{-3}	2.83
μ(Mo Kα), cm^{-1}	167.0
cryst size, mm	0.16 × 0.16 × 0.04
scan method	ω–2θ
2θ range, deg	2.5–45
scan width (2θ), deg	0.90 + 0.35 tan θ
scan rate (2θ), deg min^{-1}	0.97–2.75
colln range	$\pm h,+k,+l$
transmissn coeff range	0.112–0.576
no. of unique data	3997
no. of obsd data ($I \geq 2.5\sigma(I)$)	2163
no. of variables	189
$R_1{}^a$	0.051
$R_2{}^b$	0.057
GOF[c]	1.02
largest shift/error[d]	0.08
largest peak,[e] e $Å^{-3}$	2.2 (1)

[a] $R^1 = \sum||F_o| - |F_c||/\sum|F_o|$. [b] $R_2 = [\sum w(|F_o| - |F_c|)^2/\sum w|F_o|^2]^{1/2}$. [c] $GOF = [\sum w(|F_o| - |F_c|)^2/(N_{observns} - N_{variables})]^{1/2}$. [d] Largest shift/error in final cycle of refinement. [e] Largest peak and standard deviation in final Fourier difference map.

°C) δ 0.94 (Bu^t); ^{13}C NMR (CO region; CH_2Cl_2/CD_2Cl_2, 4/1, −101 °C) δ 200.4 (2 C), 188.7 (2 C), 186.2 (1 C), 185.5 (2 C), 180.5 (1 C), 179.6 (2 C), 175.2 (1 C), 172.9 (1 C), 171.3 (1 C), 161.7 (1 C); 2 did not give a satisfactory (EI) MS. Anal. Calcd for $C_{24}H_{18}N_2O_{14}Os_4$: C, 21.85; H, 1.38; N, 2.12. Found: C, 21.80; H, 1.57; N, 1.95.

X-ray Structure Determination of 1. Crystals of 1 of acceptable quality were grown from hexane/CH_2Cl_2; a thin plate was cleaved to suitable size (Table I) and mounted on an Enraf-Nonius CAD4F diffractometer. Diffraction data were collected at 20 ± 1 °C with the use of graphite-monochromated Mo Kα radiation (λ = 0.709 26 Å). Background measurements were made by extending the scan range by 25% on each side of the scan. Two standard reflections were monitored every hour during data collection. They indicated an approximate 10% decay of the collection period, and the data were, therefore, scaled accordingly. Accurate cell dimensions were assigned on the basis of 25 accurately centered reflections that were widely spread in reciprocal space with $24° \leq 2\theta \leq 44°$. The data were corrected for Lorentz, polarization, and absorption effects (an analytical absorption was applied).

The space group of 1 was determined to be either *P*2/*a* or *Pa* from the systematic absences. The final choice of *P*2/*a* was made after refinement: this model gave slightly better agreement with about half as many variables and was better behaved than the best model in the noncentric space group *Pa*. The osmium atoms were located by Patterson methods. All other non-hydrogen atoms were located from Fourier difference maps alternated with least-squares refinement. The methyl hydrogen atoms were placed in calculated positions (d(C–H) = 0.96 Å) and assigned a common isotropic temperature factor. The hydrogen atom positions were not refined. A common isotropic temperature factor was also assigned to the methyl carbon atoms. After anisotropic refinement of the osmium atoms an empirical weighting scheme was adopted such that $\langle w(|F_o| - |F_c|)^2\rangle$ was a nearly constant function of $|F_o|$ and $(\sin\theta)/\lambda$. The parameter w was given by $[0.904\,77t_0(x) + 0.770\,416t_1(x) + 0.376\,869t_2(x)]^{-1}$ where $x = |F_o|/F_{max}$ and t_n are polynomial functions of the Chebyshev series.[6] A disordered partial solvent molecule of CH_2Cl_2 could not be modelled in a chemically reasonable way. This, along with the decay of the intensity standards noted above, suggests that the composition of the crystal may have changed due to loss of CH_2Cl_2 during the course of the data collection. As a result of these problems the final agreement (0.051) was not as good as those we have normally obtained in the structures of other osmium clusters. We do, however, feel that the atomic parameters for 1 are satisfactory. Final convergence was achieved by full-matrix least-squares refinement. Crystallographic data and details of the data collection are given in Table I, atomic coordinates in Table II, and bond length and angle data in Table III. Neutral-atom scattering factors with anomalous dispersion corrections were employed.[7] The computer programs used were the system of the National Research Council[2] and "The CRYSTALS Program";[8] the SNOOPI program[9] was used to draw the atomic thermal ellipsoid diagram.

Table II. Fractional Coordinates for $Os_4(CO)_{15}(CNBu^t) \bullet 0.4CH_2Cl_2$ (1)

atom	*x*/*a*	*y*/*b*	*z*/*c*
Os(1)	0.36655 (8)	0.0011 (1)	0.16448 (9)
Os(2)	0.48696 (9)	0.1842 (1)	0.20747 (8)
Os(3)	0.57070 (9)	0.4028 (1)	0.22690 (9)
Os(4)	0.40157 (8)	0.4003 (1)	0.15883 (9)
N	0.405 (2)	−0.124 (3)	0.333 (2)
O(11)	0.242 (2)	−0.182 (3)	0.107 (2)
O(12)	0.240 (2)	0.159 (3)	0.242 (2)
O(13)	0.349 (1)	0.128 (2)	0.004 (2)
O(14)	0.529 (2)	−0.119 (2)	0.122 (1)
O(21)	0.560 (2)	0.144 (2)	0.043 (2)
O(22)	0.405 (2)	0.175 (3)	0.369 (2)
O(23)	0.631 (2)	0.047 (3)	0.283 (2)
O(31)	0.637 (1)	0.397 (2)	0.058 (2)
O(32)	0.506 (2)	0.396 (3)	0.396 (2)
O(33)	0.739 (2)	0.316 (3)	0.286 (2)
O(34)	0.596 (2)	0.663 (3)	0.237 (2)
O(41)	0.461 (1)	0.360 (2)	−0.012 (2)
O(42)	0.329 (2)	0.411 (3)	0.325 (2)
O(43)	0.226 (2)	0.347 (3)	0.093 (2)
O(44)	0.404 (2)	0.667 (3)	0.151 (2)
C(11)	0.289 (2)	−0.113 (4)	0.130 (2)
C(12)	0.285 (2)	0.102 (4)	0.209 (2)
C(13)	0.357 (2)	0.074 (3)	0.064 (2)
C(14)	0.473 (2)	−0.080 (3)	0.135 (2)
C(15)	0.393 (2)	−0.080 (3)	0.270 (2)
C(21)	0.533 (2)	0.163 (3)	0.103 (2)
C(22)	0.436 (2)	0.186 (4)	0.303 (2)
C(23)	0.571 (3)	0.098 (4)	0.251 (3)
C(31)	0.609 (2)	0.402 (3)	0.115 (2)
C(32)	0.531 (3)	0.399 (4)	0.326 (3)
C(33)	0.672 (3)	0.347 (4)	0.260 (3)
C(34)	0.589 (3)	0.554 (4)	0.233 (3)
C(41)	0.444 (2)	0.378 (3)	0.052 (2)
C(42)	0.358 (2)	0.405 (3)	0.266 (2)
C(43)	0.296 (2)	0.368 (3)	0.120 (2)
C(44)	0.397 (2)	0.565 (4)	0.150 (2)
C(1)	0.432 (2)	−0.186 (4)	0.404 (2)
C(2)	0.519 (3)	−0.145 (5)	0.427 (3)
C(3)	0.426 (4)	−0.316 (5)	0.392 (3)
C(4)	0.373 (3)	−0.146 (5)	0.464 (3)
Cl(1)	0.172 (2)	0.439 (3)	0.460 (2)
Cl(2)	0.2500	0.54 (1)	0.5000
Cl(3)	0.2500	0.321 (8)	0.5000

Results and Discussion

Addition of *tert*-butyl isocyanide to a CH_2Cl_2 solution of $Os_4(CO)_{15}$ at 0 °C affords $[(OC)_4(Bu^tNC)Os]Os_3(CO)_{11}$ (1) in excellent yield (eq 1). The compound is an orange, air-stable, crystalline solid. The infrared spectrum of 1 in hexane shows only terminal CO stretches. This is

---

(6) Carruthers, J. R.; Watkin, D. J. *Acta Crystallogr. Sect. A.: Cryst. Phys., Diffr., Theor. Gen. Crystallogr.* **1979**, *A35*, 698.

(7) *International Tables for X-ray Crystallography*; Kynoch: Birmingham, England, 1974; Vol. IV, Tables 2.2B and 2.3.1.

(8) Watkin, D. J.; Carruthers, J. R.; Betteridge, P. W. *CRYSTALS User Guide*; Chemical Crystallography Laboratory, University of Oxford: Oxford, 1985.

(9) Davies, E. K. *SNOOPI Plot Program*; Chemical Crystallography Laboratory, University of Oxford: Oxford, 1984.

$$Os_4(CO)_{15} + CNBu^t \xrightarrow{0\ ^\circ C} \underset{1}{[(OC)_4(Bu^tNC)Os]Os_3(CO)_{11}} \qquad (1)$$

consistent with the solid-state structure, reported below, that has no bridging carbonyl ligands.

In an independent study[10] we have prepared $Os(CO)_4(CNBu^t)$ and find the CN stretch of this compound in hexane occurs at 2190 cm^{-1}. In 1 (in hexane) the corresponding absorption is at 2200 cm^{-1}. This shift to higher frequency is consistent with removal of electron density from the osmium atom of the $Os(CO)_4(CNBu^t)$ upon coordination with a consequent decrease in the back-bonding between the metal d orbitals and the π^* orbitals of the isocyanide substituent.

Structure of 1. A view of the molecular structure of 1 is given in Figure 1; bond lengths and angles are given in Table III. As can be seen from the figure, the cluster has the spiked triangular geometry in which the 18-electron complex $Os(CO)_4(CNBu^t)$ acts as two-electron donor ligand toward the $Os_3(CO)_{11}$ fragment. The osmium atom of the $Os(CO)_4(CNBu^t)$ ligand lies 0.100 (3) Å above the plane formed by the other three osmium atoms. This deviation from planarity is away from that side of the plane with the $CNBu^t$ ligand and may be the result of steric interactions between the more bulky isocyanide ligand and the carbonyls CO(22) and CO(23) on Os(2). The donor–acceptor metal–metal bond is unbridged which is also the case in the related clusters $[(Me_3P)(OC)_4Os]Os_3(CO)_{11}$ (4)[2] and $\{[MeC(CH_2O)_3P](OC)_4Os\}Os_3(CO)_{11}$ (5).[11]

Somewhat surprisingly the isocyanide ligand is cis rather than trans to the donor–acceptor Os–Os bond. In the four complexes, which includes 4, that we have structurally characterized and which have $Os(CO)_4(PMe_3)$ as a ligand, the phosphine substituent is trans to the dative metal–metal bond.[2,12,13] The phosphite group is also trans to the dative Os–Os bond in 5.[11] There is spectroscopic evidence for the cis isomer for some of the $Os(CO)_4(PMe_3)$ derivatives in solution.[12] The reason for the site preference of the non-carbonyl group in these complexes is at present not clear. Both PMe_3 and $CNBu^t$ are considered better σ-donors but poorer π-acceptors than CO.[14] It may be that the cis position is electronically preferred for the non-carbonyl ligands, since it avoids as far as possible carbonyls competing for the same π-electron density on the metal atom. Steric interactions, however, could force the PMe_3 (or $P(OCH_2)_3CMe$) group to adopt the site trans to the metal–metal bond. It is interesting that a similar situation occurs in triosmium carbonyl clusters: phosphorus donor ligands adopt equatorial sites,[15,16] but isocyanide ligands are found in axial positions.[17,18]

Table III. Bond Lengths and Selected Angles for 1

Bond Lengths (Å)

Os(1)-Os(2)	2.918 (2)	C(11)-O(11)	1.15 (5)
Os(2)-Os(3)	2.853 (2)	C(12)-O(12)	1.13 (4)
Os(2)-Os(4)	2.929 (2)	C(13)-O(13)	1.18 (3)
Os(3)-Os(4)	2.890 (2)	C(14)-O(14)	1.03 (3)
Os(1)-C(11)	1.88 (4)	C(15)-N	1.17 (4)
Os(1)-C(12)	1.92 (4)	C(21)-O(21)	1.14 (4)
Os(1)-C(13)	1.88 (3)	C(22)-O(22)	1.22 (4)
Os(1)-C(14)	2.01 (3)	C(23)-O(23)	1.23 (5)
Os(1)-C(15)	2.04 (4)	C(31)-O(31)	1.07 (4)
Os(2)-C(21)	1.83 (4)	C(32)-O(32)	1.24 (5)
Os(2)-C(22)	1.94 (3)	C(33)-O(33)	1.19 (5)
Os(2)-C(23)	1.80 (5)	C(34)-O(34)	1.26 (5)
Os(3)-C(31)	2.00 (4)	C(41)-O(41)	1.14 (3)
Os(3)-C(32)	1.81 (4)	C(42)-O(42)	1.12 (4)
Os(3)-C(33)	1.81 (4)	C(43)-O(43)	1.21 (4)
Os(3)-C(34)	1.76 (5)	C(44)-O(44)	1.18 (5)
Os(4)-C(41)	1.96 (3)	N-C(1)	1.44 (5)
Os(4)-C(42)	1.95 (3)	C(1)-C(2)	1.50 (5)
Os(4)-C(43)	1.82 (4)	C(1)-C(3)	1.50 (6)
Os(4)-C(44)	1.89 (4)	C(1)-C(4)	1.48 (5)

Angles (deg)

Os(1)-Os(2)-Os(3)	164.02 (6)	C(21)-Os(2)-C(23)	90 (2)
Os(1)-Os(2)-Os(4)	104.17 (6)	C(31)-Os(3)-C(32)	177 (2)
Os(3)-Os(2)-Os(4)	59.96 (5)	C(31)-Os(3)-C(33)	89 (2)
Os(2)-Os(3)-Os(4)	61.32 (5)	C(33)-Os(3)-C(34)	100 (2)
Os(2)-Os(4)-Os(3)	58.72 (5)	C(41)-Os(4)-C(42)	174 (2)
C(11)-Os(1)-Os(2)	176 (1)	C(41)-Os(4)-C(43)	90 (2)
C(11)-Os(1)-C(12)	95 (2)	C(43)-Os(4)-C(44)	98 (2)
C(12)-Os(1)-Os(2)	86 (1)	C(15)-N-C(1)	170 (4)
C(12)-Os(1)-C(13)	93 (2)	N-C(1)-C(2)	108 (4)
C(12)-Os(1)-C(14)	165 (2)	N-C(1)-C(3)	112 (4)
C(13)-Os(1)-C(15)	173 (2)	N-C(1)-C(4)	103 (4)
C(21)-Os(2)-C(22)	172 (2)		

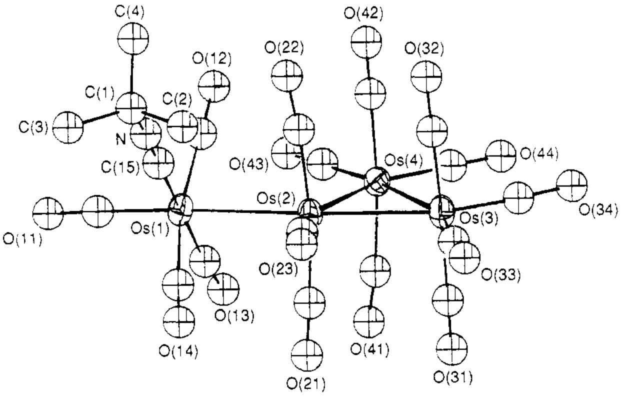

Figure 1. Molecular structure of $Os_4(CO)_{15}(CNBu^t)$ (1).

The dative Os–Os bond in 1 is 2.918 (2) Å whereas in 4 it is 2.938 Å (mean of two independent lengths) which suggests the dative bond is slightly stronger in the former molecule. This is contrary to expectation since the donor ability of $Os(CO)_4(PMe_3)$ should be greater than that of $Os(CO)_4(CNBu^t)$ because PMe_3 is a better donor than $CNBu^t$. It may indicate that there is indeed a weakening of the dative metal–metal bond by having the non-carbonyl ligand PMe_3 trans to this bond. The Os–Os bond lengths within the osmium triangle show significant differences (Table III). The corresponding lengths in 4 show virtually identical variations.[2]

---

(10) Batchelor, R. J.; Einstein, F. W. B.; Pomeroy, R. K.; Shipley, J. A., to be submitted for publication.

(11) Einstein, F. W. B.; Johnston, V. J.; Ma, A. K.; Pomeroy, R. K., to be submitted for publication.

(12) (a) Einstein, F. W. B.; Jones, T.; Pomeroy, R. K.; Rushman, P. *J. Am. Chem. Soc.* **1984**, *106*, 2707. (b) Davis, H. B.; Einstein, F. W. B.; Glavina, P. G.; Jones, T.; Pomeroy, R. K.; Rushman, P. *Organometallics* **1989**, *8*, 1030.

(13) Einstein, F. W. B.; Jennings, M. C.; Krentz, R.; Pomeroy, R. K.; Rushman, P.; Willis, A. C. *Inorg. Chem.* **1987**, *26*, 1341.

(14) (a) Cotton, F. A.; Wilkinson, G. *Advanced Inorganic Chemistry*, 5th ed.; Wiley: New York, 1988; p 62. (b) Greenwood, N. N.; Earnshaw, A. *Chemistry of the Elements*; Pergamon: New York, 1984; p 349.

(15) For example (a) Dahm, D. J.; Jacobson, R. A. *J. Am. Chem. Soc.* **1968**, *90*, 5106. (b) Churchill, M. R.; DeBoer, B. G. *Inorg. Chem.* **1977**, *16*, 2397. (c) Benfield, R. E.; Johnson, B. F. G.; Raithby, P. R.; Sheldrick, G. M. *Acta Crystallogr., Sect. B: Struct. Crystallogr. Cryst. Chem.* **1978**, *B34*, 666. (d) Bruce, M. I.; Matisons, J. G.; Skelton, B. W.; White, A. H. *J. Chem. Soc., Dalton Trans.* **1983**, 2375. (e) Venäläinen, T.; Pakkanen, T. A. *J. Organomet. Chem.* **1984**, *266*, 269. (f) Alex, R. F.; Einstein, F. W. B.; Jones, R. H.; Pomeroy, R. K. *Inorg. Chem.* **1987**, *26*, 3175. (g) Bruce, M. I.; Liddel, M. J.; Hughes, C. A.; Skelton, B. W.; White, A. H. *J. Organomet. Chem.* **1988**, *347*, 157.

(16) Johnson, B. F. G.; Lewis, J.; Reichert, B. E.; Schorpp, K. T. *J. Chem. Soc., Dalton Trans.* **1976**, 1403.

(17) (a) Mays, M. J.; Gavens, P. D. *J. Chem. Soc., Dalton Trans.* **1980**, 911. (b) Bruce, M. I.; Matisons, J. G.; Wallis, R. C.; Patrick, J. M.; Skelton, B. W.; White, A. H. *J. Chem. Soc., Dalton trans.* **1983**, 2365.

(18) (a) Adams, R. D.; Golembeski, N. M. *Inorg. Chem.* **1979**, *18*, 1909. (b) Adams, R. D.; Golembeski, N. M. *J. Am. Chem. Soc.* **1979**, *101*, 2579.

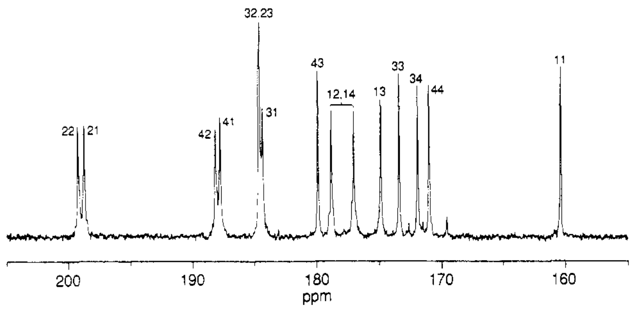

Figure 2. ^{13}C NMR spectrum of 1 at −118 °C (^{13}CO-enriched sample; $CHFCl_2/CD_2Cl_2$ solution; 100.6-MHz operating frequency). The assignment of the signals follows the labeling in Figure 1.

Other structures reported in the literature that contain the $OsCNBu^t$ unit are the red[18] and green[19] isomers of $Os_3(\mu\text{-}H)_2(CO)_9(CNBu^t)$, $HOs_3(\mu\text{-}H)(CO)_{10}(CNBu^t)$,[18] and $Os_4(CO)_n(CNBu^t)(\mu_3\text{-}S)_2$ (n = 11, 12).[20] The dimensions of the $OsCNBu^t$ unit in 1 do not show any unusual features when compared to the corresponding dimensions reported for these structures.

The reasons why 1 and 4 have spiked triangular metal cores whereas 3 has a cyclobutane-like skeleton is not clear but can probably be attributed to electronic effects since the steric effects of CO and $CNBu^t$ are expected to be similar. Further studies on clusters of the type $Os_4(CO)_{15}(L)$ are in progress. (Molecular orbital calculations are also planned in order to understand why these clusters adopt different metal frameworks.) It should be pointed out here that 1 is formed by the addition of CO to $Os_4(CO)_{14}(CNBu^t)$ (which has a similar metal framework to $Os_4(CO)_{15}$[11]). This indicates the spiked triangular geometry is the thermodynamically stable form of 1.

Nonrigidity in 1. The ^{13}C NMR spectrum of 1 (^{13}CO enriched) in $CHFCl_2/CD_2Cl_2$ at −118 °C exhibits 14 carbonyl resonances, each of approximate intensity of 1 except the resonance at δ 184.6 which has an intensity of 2 (Figure 2). The spectrum at −108 °C (not shown) indicates that this signal is comprised of two signals. Fifteen resonances are consistent with the solid-state structure for 1 if the isocyanide group remains locked to one side of the Os_4 plane in solution (this is discussed in detail below). From the spectrum in Figure 2, it can be seen that there is no real evidence for a second isomer of 1 with the $CNBu^t$ group trans to the dative Os–Os bond or with the $CNBu^t$ occupying a site on the Os_3 triangle. This latter observation probably means the $CNBu^t$ ligand does not migrate across the dative Os–Os bond as CO does (see below).

The assignments of the signals shown in Figure 2 follows the labeling scheme in Figure 1. The assignment is based on the following: The resonance of a carbonyl with a chemically different carbonyl trans to it is expected to show C–C coupling;[21] the resonances of axial carbonyls appear to lower field to those of the corresponding equatorial carbonyls of $Os(CO)_4$ or $Os(CO)_3(L)$ units in osmium clusters;[22,23] the resonances of $Os(CO)_3(L)$ groups come to lower field than the corresponding resonances of $Os(CO)_4$ groups;[22,23] for axial carbonyls attached to the same osmium atom the carbonyl nearest the $CNBu^t$ ligand gives rise to the resonance further downfield;[19] the resonance of the carbonyl trans to the dative metal–metal bond appears at characteristic high fields;[12,24] the mode of collapse of the signals at higher temperatures and the proposed mechanism for the collapse (discussed below).

Chart I

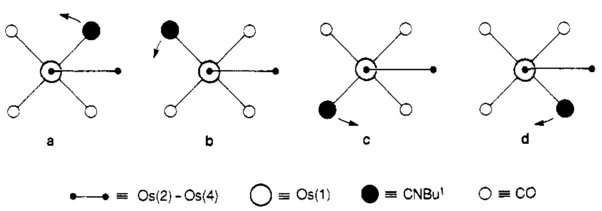

Chart II

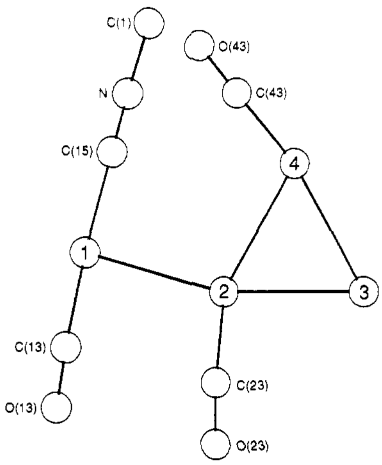

Chart III

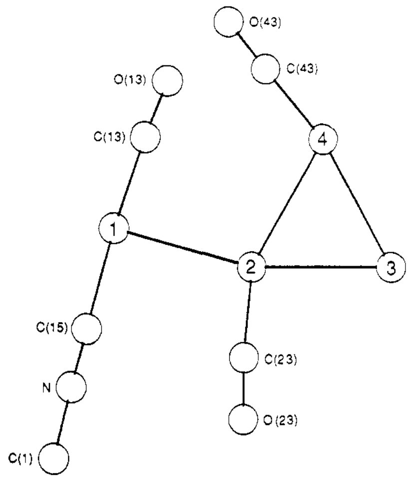

As mentioned the spectrum of 1 at low temperature indicates the $CNBu^t$ is locked in a position not in the Os_4 plane, that is, the rotation about the Os(1)–Os(2) bond is slow on the NMR time scale. Chart I is a diagrammatic representation of the various staggered conformers that result from rotation about the Os(1)–Os(2) bond. Models show there is a severe steric interaction between the isocyanide ligand and the vicinal equatorial carbonyl on Os(4) (i.e., CO(43)) when the Os(1)–Os(2) bond is rotated (Chart

---

[19] Ma, A. K.; Einstein, F. W. B.; Johnston, V. J.; Pomeroy, R. K. *Organometallics*, preceding paper in this issue.

[20] Adams, R. D.; Horváth, I. T.; Natarajan, K. *Organometallics* **1984**, *3*, 1540.

[21] (a) Tachikawa, M.; Richter, S. I.; Shapley, J. R. *J. Organomet. Chem.* **1977**, *128*, C9. (b) Aime, S.; Osella, D. *J. Chem. Soc., Chem. Commun.* **1981**, 300.

[22] (a) Mann, B. E.; Taylor, B. F. *^{13}C NMR Data for Organometallic Compounds*; Academic: New York, 1981; p 176. (b) Aime, S.; Osella, D.; Milone, L.; Rosenberg, E. *J. Organomet. Chem.* **1981**, *213*, 207.

[23] Alex, R. F.; Pomeroy, R. K. *Organometallics* **1987**, *6*, 2437.

[24] (a) Einstein, F. W. B.; Pomeroy, R. K.; Rushman, P.; Willis, A. C. *J. Chem. Soc., Chem. Commun.* **1983**, 854. (b) Fleming, M. M.; Pomeroy, R. K.; Rushman, P. *J. Organomet. Chem.* **1984**, *273*, C33.

Scheme I

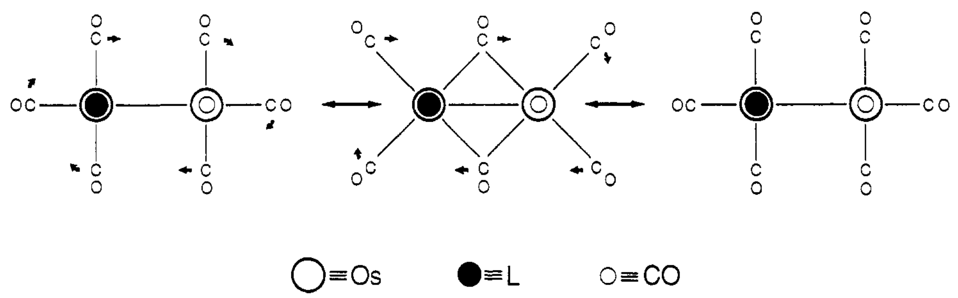

II).[25] It is easy to visualize that this interaction could prevent the direct conversion of the conformers represented as **a** and **d**. This is, however, not sufficient to account for the inequivalencies in the low-temperature ^{13}C NMR spectrum of **1** since rapid oscillation back and forth between conformers **a** and **d** via conformers **b** and **c** (i.e., without the $CNBu^t$ ligand passing CO(43)) would result in the pairs of carbonyls above and below the Os_4 plane becoming equivalent (which is observed at higher temperatures). If the barrier to rotation is steric in origin, there must be a second point of severe steric interaction to cause the inequivalencies. This could be due to either the $CNBu^t$ ligand passing a second carbonyl (CO(21), CO(22), or CO(23)) or to a radial carbonyl of $Os(CO)_4(CNBu^t)$ passing the vicinal carbonyl CO(43). Models show that it is probably the latter interaction that gives rise to the barrier (Chart III).

If the barrier to rotation or oscillation is due to a carbonyl of the $Os(CO)_4(L)$ ligand passing a vicinal equatorial carbonyl of the $Os_3(CO)_{11}$ unit, then a similar barrier should be present in $(Me_3P)(OC)_4OsOs_3(CO)_{11}$ (**4**). Such a barrier could be detectable since the ^{13}C NMR signal due to the radial carbonyls should be split into two due to inner (near the Os_3 triangle) and outer pairs. We therefore investigated the ^{13}C NMR spectrum of **4** at lower temperatures than our previous study,[2] but the results were inconclusive. At −90 °C the signal assigned to the radial carbonyls of the $Os(CO)_4(PMe_3)$ unit was slightly broadened which might have indicated the onset of restricted rotation about the Os–Os dative bond. Studies at still lower temperatures were prevented by the low solubility of the compound. It might be expected that the barrier to this rotation in **4** would be lower than the corresponding barrier in **1** since the dative Os–Os bond length in **4** is somewhat longer than that in **1**.

On warming the sample of **1** from −110 to −50 °C, four pairs of signals each coalesce to a singlet (Figure 3). This behavior is, of course, consistent with the onset of oscillation of the $CNBu^t$ group about the Os_4 plane. Given the severity of the interaction between the $CNBu^t$ ligand with CO(43) (Chart II), it is probable that there is never completely free rotation about the Os(1)–Os(2) bond. Simulation of the spectrum at −85 ± 2 °C (Figure 4) yielded a first-order rate constant for the process of 350 ± 35 s^{-1} which corresponds to a $\Delta G^{\ddagger} = 8.7 \pm 0.2$ kcal mol^{-1}. The only other examples that we are aware of in the literature of restricted rotation about unbridged, single bonds between transition metals are those in molecules of the type $[(\eta^5\text{-}C_5H_5)M(CO)_3]_2$ (M = Cr, Mo, W) and the related $(\eta^5\text{-}C_5H_5)_2Mo_2(CO)_5(CNMe)$ observed by Cotton and coworkers.[26]

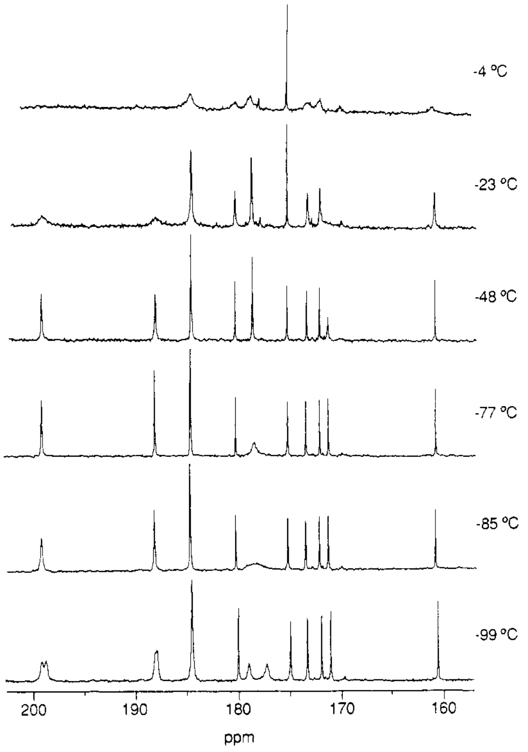

Figure 3. Variable-temperature ^{13}C NMR spectra of **1** (conditions as in Figure 2).

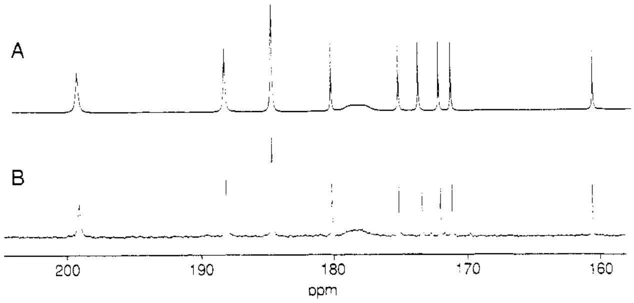

Figure 4. Calculated (A) and observed (B) ^{13}C NMR spectra for **1** at −85 °C.

From about −50 to −20 °C, two signals assigned to equatorial carbonyls and two signals assigned to axial carbonyls of the $Os_3(CO)_{11}$ unit collapse to the base line (Figure 3; one of the resonances is degenerate with a signal at δ 184.7 that does not collapse). Of the latter two signals, one is due to the axial carbonyls attached to the osmium atom to which the $Os(CO)_4(CNBu^t)$ group is bound. This pattern of collapse has been observed previously in **4**[2] and other $Os_3(CO)_{11}(L)$ derivatives;[16,23] it has been rationalized in terms of the well-known, terminal–bridge carbonyl exchange in the axial plane that is cis perpendicular to L as shown in Scheme I (L = $Os(CO)_4(CNBu^t)$). Simulation

---

[25] The C(1)···O(43) distance in the conformation shown in Chart II is estimated to be 1.05 Å.

[26] Mann, B. E. In *Comprehensive Organometallic Chemistry*; Wilkinson, G., Stone, F. G. A., Abel, E. W., Eds.; Pergamon: Oxford, 1982; Vol. 3, p 89 (see p 104) and references therein.

Scheme II

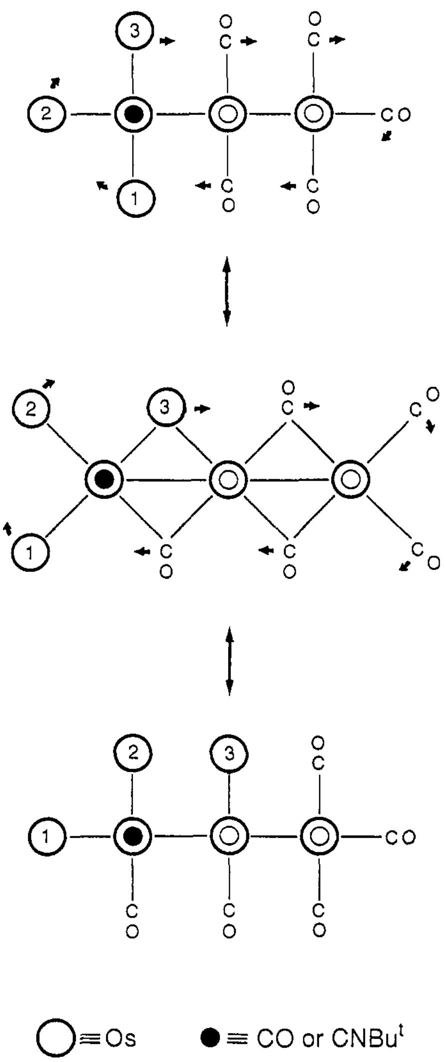

of the spectrum at −48 ± 2 °C gave a first-order rate constant for this process of 11 ± 1 s^{-1} and hence $\Delta G^{\ddagger}$ = 12.0 ± 0.2 kcal mol^{-1}.

Between −20 and −4 °C all the remaining signals except that at δ 174.9 collapsed to the base line (Figure 3). Spectra at higher temperatures were not investigated because of appreciable decomposition of the sample in solution at these temperatures. We believe this behavior is best rationalized in terms of terminal–bridge carbonyl exchanges, with approximately equal activation energies, in the other two planes that are perpendicular to the Os$_4$ plane and pass through two of the osmium atoms of the Os$_3$ triangle. Furthermore, three of the four carbonyls of the Os(CO)$_4$(CNBu^t) grouping are believed take part in the exchange in the plane that contains Os(2) and Os(3); this is shown in Scheme II (positions 1, 2, and 3 occupied by CO). The sharp signal in the spectrum of the sample at −4 °C is therefore assigned to the carbonyl trans to the CNBu^t ligand (i.e., CO(13)).

A similar exchange was proposed for 4; however, the noncarbonyl ligand in this molecule is initially trans to the metal–metal bond (i.e., in position 2), and isomerization occurs with the terminal–bridge carbonyl exchange. This isomerization results in all the carbonyls of 4 becoming involved in the exchange and all the signals of the Os(CO)$_4$(PMe$_3$) unit collapse, as observed. That one of the signals of the Os(CO)$_4$(CNBu^t) grouping remains sharp probably indicates that the isomer of 1 with the CNBu^t trans to the Os(1)–Os(2) bond is not present in solution.

Chart IV

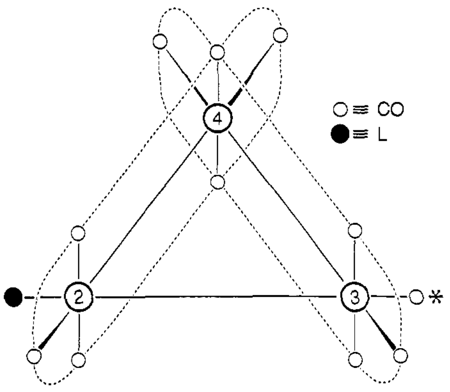

Strong support for this view is provided by the fluxional processes exhibited by [(OC)$_3$(Bu^{t}NC)$_2$Os]Os$_3$(CO)$_{11}$ reported below.

It is pointed out here that in Os$_3$(CO)$_{11}$[P(OMe)$_3$] terminal–bridge carbonyl exchange occurs in only two of the axial planes as shown in Chart IV (L = P(OMe)$_3$). This results in all the ^{13}C NMR signals except one (that marked with an asterisk) of the Os$_3$(CO)$_{11}$ unit collapsing to the base line.[23] (The low-temperature ^{13}C NMR spectrum of Ru$_3$(CO)$_{11}$[P(OMe)$_3$] exhibits two signals in a 10:1 ratio which indicates the same processes are probably occurring but at a faster rate.[27]) That a similar situation could be taking place in 1 was therefore considered, that is, the sharp signal in the spectrum recorded with the sample at −4 °C is due to the carbonyl in the trans, three-bond position to the Os(CO)$_4$(CNBu^t) ligand (i.e., Chart IV, L = Os(CO)$_4$(CNBu^t)). This was, however, rejected as improbable. Since at least two of the carbonyl signals of the Os(CO)$_4$(CNBu^t) grouping collapse simultaneously with some of the signals due to carbonyls of the Os$_3$(CO)$_{11}$ moiety, we believe that the various carbonyls are involved in the same exchange process rather than two independent processes. If the mechanism shown in Chart IV is applied to 1 (i.e., no exchange in the axial Os(1)–Os(2)–Os(3) plane so that CO(34) remains rigid), it would require all three different types of carbonyls of the Os(CO)$_4$(CNBu^t) unit to simultaneously exchange with some of the carbonyls attached to Os(4), an atom that is not directly bound to the Os(CO)$_4$(CNBu^t) fragment. We consider this most unlikely.

Further support for the mechanism shown in Scheme II over that shown in Chart IV comes from the fluxional processes exhibited by [(OC)$_3$(Bu^{t}NC)$_2$Os]Os$_3$(CO)$_{11}$ discussed in detail below. The mechanism in Scheme II also leads to the assignment of the carbonyl resonance trans to the CNBu^t ligand (CO(13)) as upfield rather than downfield to the signal due to the carbonyls cis to the isocyanide ligand (CO(12) and CO(14)). In (OC)$_4$(Bu^{t}NC)OsCr(CO)$_5$, recently prepared in our laboratory and where the assignment of the ^{13}C NMR resonances is unambiguous,[10] the signal of the carbonyl trans to CNBu^t is also to higher field than the resonances of the carbonyls cis to the CNBu^t ligand (but not trans to the dative Os–Cr bond).

If the process in Scheme II is operative in 1, then exchange must also occur in the axial plane containing the Os(3) and Os(4) atoms in order that all the signals due to the carbonyls of the Os$_3$(CO)$_{11}$ moiety collapse. This, however, is expected: the corresponding exchanges in the allowed planes of Os$_3$(CO)$_{12-x}$[P(OMe)$_3$]$_x$ (x = 1, 2, 4)[23] and

---

[27] Deeming, A. J. *Adv. Organomet. Chem.* **1986**, *26*, 1 (see p 47).

Chart V

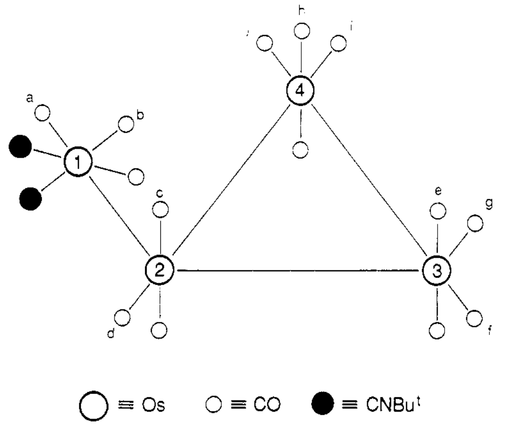

in $Os_3(CO)_{12-x}(PEt_3)_x$ (x = 1, 2)[16] have similar activation energies.

Synthesis and Fluxional Properties of $Os_4(CO)_{14}(CNBu^t)_2$ (2). The cluster 2 was prepared by the addition of $CNBu^t$ to $Os_4(CO)_{14}$[4] in solution at room temperature (eq 2). There was no evidence in the infrared spectrum

$$Os_4(CO)_{14} + 2CNBu^t \rightarrow \underset{\mathbf{2}}{Os_4(CO)_{14}(CNBu^t)_2} \quad (2)$$

of the reaction mixture for the intermediate formation of $Os_4(CO)_{14}(CNBu^t)$ (6). (We have, however, prepared 6 by the addition of Me_3NO to 1.[11]) The failure to observe the intermediate formation of 6 indicates that the reaction of 6 with $CNBu^t$ is faster than the initial addition of isocyanide to $Os_4(CO)_{14}$.

The product 2 is an air-stable, orange, crystalline solid. The ^{13}C NMR spectrum of the cluster, which is discussed in detail below, indicates it has the structure shown in Chart V. Consistent with this structure is that the infrared spectrum of 2 exhibits two CN stretches as expected for a cis arrangement of the isocyanide ligands.

The cis arrangement of the $CNBu^t$ ligands avoids the steric interactions of these ligands with the vicinal carbonyl (i.e., carbonyl j, Chart V). As discussed for 1, the arrangement also avoids as far as possible the better π-acceptor CO ligands competing for the same electron density on the central metal atom. The isocyanide ligands in $Re_2(CO)_{10-x}(CNR)_x$ (x = 3, 4) occupy cis-equatorial positions.[28]

The ^{13}C NMR spectrum of 2 (^{13}CO-enriched) in CH_2Cl_2/CD_2Cl_2 at −101 °C is shown in Figure 5. As previously stated, the spectrum is consistent with the structure shown in Chart V; as found for 1, there is no evidence for a second isomer of 2 in solution. The assignment of the signals shown in Chart V and Figure 5 follows arguments similar to those previously discussed for 1. The assignments of the resonances labeled f, g, and j is not as definitive as the assignment of the other signals. It is based on the assumption that peaks due to carbonyls in similar chemical environments (in both 1 and 2) should have similar chemical shifts.

Because of the cis arrangement of the $CNBu^t$ ligands, the radial carbonyls of the $Os(CO)_3(CNBu^t)_2$ ligand are chemically equivalent. For this reason, it is impossible to detect by NMR spectroscopy whether there is restricted rotation about the Os–Os dative bond. It would be expected that the barrier to oscillation (and rotation) about the Os–Os dative bond in 2 would be at least as great as that in 1.

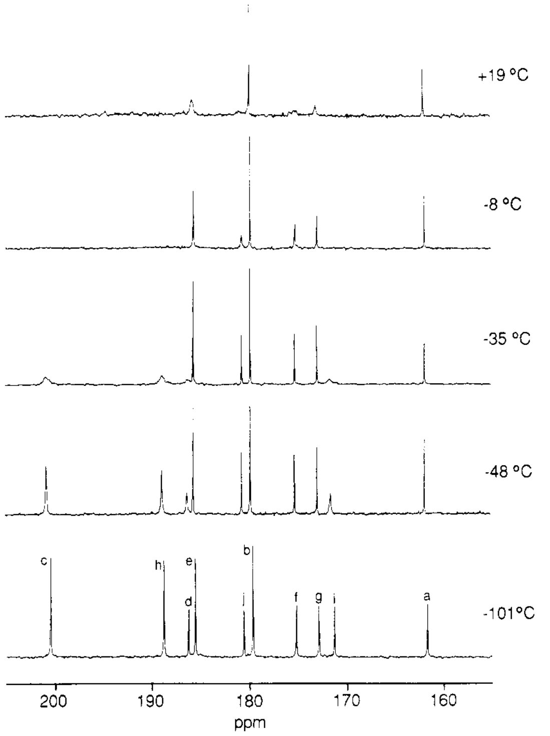

Figure 5. Variable-temperature ^{13}C NMR spectra for $Os_4(CO)_{14}(CNBu^t)_2$ (^{13}CO-enriched sample; CD_2Cl_2 solution; 100.6-MHz operating frequency). The assignment of the signals is given in Chart V.

When the solution of 2 is warmed to above −60 °C, the signals labeled c, d, h, and i collapse to the base line. This now familiar behavior for $Os_3(CO)_{11}(L)$ clusters is interpreted in terms of terminal–bridge carbonyl exchange in the axial plane of the Os_3 triangle that contains Os(2) and Os(4) (i.e., as in Chart IV, L = $Os(CO)_3(CNBu^t)_2$). Simulation of the spectrum at −48 ± 2 °C yielded a first-order rate constant of 14 ± 2 s^{-1} and hence a ΔG^* of 11.9 ± 0.2 kcal mol^{-1}.

Warming the sample of 2 to above −10 °C causes four more of the signals to broaden and collapse to the base line (Figure 5). The two remaining sharp signals stay sharp even in the spectrum at room temperature. These signals can be confidently assigned to the two types of carbonyls of the $Os(CO)_3(CNBu^t)_2$ ligand on the basis of their intensities and chemical shifts. Whereas some of the carbonyls of the $Os(CO)_4(CNBu^t)$ unit in 1 can exchange with those of the $Os_3(CO)_{11}$ grouping as in Scheme II, the analogous exchange does not occur in 2. If position 1 in Scheme II, is occupied by an isocyanide ligand, then for the exchange shown in the scheme to occur it would require the $CNBu^t$ group to move to an axial position. That this apparently does not occur suggests there is a strong electronic preference for the $CNBu^t$ substituent to remain in a radial position. If, on the other hand, position 3 in Scheme II is occupied by an isocyanide ligand, then an intermediate with a bridging isocyanide ligand (and bridging CO) is required for the exchange to occur. That this also apparently does not occur indicates that this intermediate has a higher energy than the corresponding intermediate with two bridging carbonyls. It may be that the π* orbitals on $CNBu^t$ are higher in energy than those on CO (since the NBu^t unit is less electronegative than an oxygen atom), and therefore, there may not be good overlap of these orbitals with the filled d orbitals on the adjacent osmium atom to allow ready formation of the

---

[28] (a) Harris, G. W.; Coville, N. J. *Organometallics* **1985**, *4*, 908. (b) Harris, G. W.; Boeyens, J. C. A.; Coville, N. J. *Ibid.* **1985**, *4*, 914.

bridged intermediate in the case of CNBu^t. The failure of the CNBu^t ligand to bridge the Os–Os dative bond in **1** also accounts for why the carbonyl trans to this ligand does not undergo ready exchange with the rest of the carbonyls in the molecule.

As can be seen from Figure 5 all the carbonyls of the Os$_3$(CO)$_{11}$ unit undergo exchange at 19 °C. Terminal-bridge carbonyl exchange in the perpendicular plane that contains Os(3) and Os(4) can account for the collapse of the signals attributed to carbonyls e, f, and j. There must, however, be an additional rearrangement in **2** in order that the signal assigned to carbonyl g can collapse. This may be a 3-fold twist at Os(3) that exchanges carbonyls e, f, and g. This type of exchange has been proposed for Os$_3$(CO)$_{12-x}$[P(OMe)$_3$]$_x$ (x = 1–5).[23,29] There was some evidence that such an exchange occurs at Os(4) in that the signal assigned to carbonyl j collapsed to the base line at a rate faster than expected if this carbonyl were only involved in the CO exchange in the perpendicular plane containing Os(3) and Os(4). This is apparent in the spectrum at −8 °C (Figure 5) since the signals f and j should collapse at the same rate if they are only involved in one rearrangement.

Acknowledgment. We thank the Natural Sciences and Engineering Research Council of Canada and Simon Fraser University for financial support.

Registry No. 1, 123724-38-9; 2, 123724-39-0; Os$_4$(CO)$_{15}$, 110698-51-6; Os$_4$(CO)$_{14}$, 115227-28-6; Os, 7440-04-2.

Supplementary Material Available: Tables of hydrogen atom coordinates and anisotropic thermal parameters for **1** (2 pages); a listing of observed and calculated structure factors for **1** (14 pages). Ordering information is given on any masthead page.

---

(29) Alex, R. F.; Pomeroy, R. K. *J. Organomet. Chem.* **1985**, *284*, 379.

Chemistry of η^2-CS$_2$ Metal Complexes. Comparison of the Reactivities of the Two Isomeric Heterometallacycles $\overline{\text{MoC(S)SC(R)=C}}\text{R}$ and $\overline{\text{MoSC(S)C(R)=C}}\text{R}$. Unexpected Formation of a Carbon–Carbon Bond between the Five-Membered Metalla Ring and an η^5-Cyclopentadienyl Ligand

Françoise Conan,[1a] Jean Sala-Pala,[1a] Jacques E. Guerchais,*,[1a] and Loïc Toupet[1b]

Laboratoire de Chimie Inorganique Moléculaire, URA CNRS 322, "Chimie et Electrochimie Moléculaires", Université de Bretagne Occidentale, 29287 Brest Cedex, France, and Groupe de Physique Cristalline, URA CNRS 804, Université de Rennes I, 35042 Rennes Cedex, France

Received February 13, 1989

Two aspects of the chemistry of the two isomeric heterometallacycles arising from 1:1 addition of alkynes to [Cp$_2$Mo(η^2-CS$_2$)], i.e. [Cp$_2\overline{\text{MoC(S)SC(R)=C}}$R] (**1a**, R = CO$_2$Me; **1b**, R = CF$_3$) and [Cp$_2\overline{\text{MoSC(S)C(R)=C}}$R] (**2a**, R = CO$_2$Me), have been studied: (i) their reactions with methyl iodide and (ii) the subsequent reactions with sodium tetrahydroborate. While CH$_3$I reacts with **1a** and **2a** to give the corresponding S-methylated cationic complexes [Cp$_2\overline{\text{MoC(SCH}_3\text{)SC(R)=C}}$R]I (**3a**, R = CO$_2$Me) and [Cp$_2\overline{\text{MoSC(SCH}_3\text{)C(R)=C}}$R]I (**4a**, R = CO$_2$Me), respectively, the reaction with **1b** affords the molecular complex [Cp$\overline{\underline{\text{Mo(}\eta^7\text{-C}_5\text{H}_4\text{C}}\text{(SCH}_3\text{)SC(R)=C}}$R)] (**5b**, R = CF$_3$). Complex **3a** reacts with sodium tetrahydroborate to give **5a**, the CO$_2$Me analogue of **5b**, and [Cp$_2\overline{\text{MoCH(SCH}_3\text{)SC(R)=C}}$R] (**6a**, R = CO$_2$Me). Complex **4a** reacts with sodium tetrahydroborate to afford [Cp$\overline{\underline{\text{Mo(}\eta^7\text{-C}_5\text{H}_4\text{C}}\text{(R)C(R)=C(SCH}_3\text{)S}}$)] (**7a**, R = CO$_2$Me) and [Cp$_2\overline{\text{MoSCH}_2\text{C(R)=C}}$R] (**8a**, R = CO$_2$Me). Possible mechanisms for these reactions are discussed. The structure of **5b** has been determined by single-crystal X-ray diffraction analysis. The crystals are monoclinic, space group $P2_1/c$, with a = 11.861 (3) Å, b = 9.839 (3) Å, c = 15.075 (4) Å, β = 106.28 (2)°, V = 1688.7 (5) Å^3, Z = 4 and D_c = 1.88 g·cm^{-3}. The structure was solved by using 2953 unique reflections ($I > 3\sigma(I)$) and refined to R = 0.027 and R_w = 0.024. This study clearly shows the unexpected formation of a carbon–carbon bond between a cyclopentadienyl group and the heterometallacyclic fragment (C–C = 1.454 (3) Å).

Introduction

The η^2-coordinated CS$_2$ ligand exhibits nucleophilic behavior, which began to be exploited in organometallic and organic synthesis a few years ago.[2] Among the different aspects of its reactivity which have been examined, the reaction with acetylenes bearing electron-withdrawing groups is one of the most investigated.[2-8] In most cases

---

(1) (a) Université de Bretagne Occidentale. (b) Université de Rennes I.

(2) For review see: Bianchini, C.; Mealli, C.; Meli, A.; Sabat, M. *Stereochemistry of Organometallic and Inorganic Compounds*; Bernal, I., Ed.; Elsevier: Amsterdam, 1986; Vol. 1, pp 146–254.

(3) Wakatsuki, Y.; Yamazaki, H.; Iwasaki, H. *J. Am. Chem. Soc.* **1973**, *95*, 5781.

(4) (a) Le Bozec, H.; Gorgues, A.; Dixneuf, P. H. *J. Chem. Soc., Chem. Commun.* **1978**, 573. (b) *J. Am. Chem. Soc.* **1978**, *100*, 3946. (c) *Inorg. Chem.* **1981**, *20*, 2486.

(5) Le Marouille, J. Y.; Lelay, C.; Benoit, A.; Grandjean, D.; Touchard, D.; Le Bozec, H.; Dixneuf, P. H. *J. Organomet. Chem.* **1980**, *191*, 133.

0276-7333/90/2309-0059$02.50/0